Neutral Silicon Vacancy Centers in Undoped Diamond via Surface Control

Zi-Huai Zhang, Josh A. Zuber, Lila V. H. Rodgers, Xin Gui, Paul Stevenson, Minghao Li, Marietta Batzer, Marcel.li Grimau Puigibert, Brendan J. Shields, Andrew M. Edmonds, Nicola Palmer, Matthew L. Markham, Robert J. Cava, Patrick Maletinsky, and Nathalie P. de Leon

Phys. Rev. Lett. **130**, 166902 — Published 21 April 2023

DOI: 10.1103/PhysRevLett.130.166902

Neutral silicon vacancy centers in undoped diamond via surface control

Zi-Huai Zhang,[1] Josh A. Zuber,[2,3] Lila V. H. Rodgers,[1] Xin Gui,[4] Paul Stevenson,[5] Minghao Li,[2,3] Marietta Batzer,[2,3] Marcel.li Grimau,[2,3] Brendan Shields,[2,3] Andrew M. Edmonds,[6] Nicola Palmer,[6] Matthew L. Markham,[6] Robert J. Cava,[4] Patrick Maletinsky,[2,3] and Nathalie P. de Leon[1,*]

[1] *Department of Electrical and Computer Engineering, Princeton University, Princeton, New Jersey 08544, USA*
[2] *Department of Physics, University of Basel, Klingelbergstrasse 82, 4056 Basel, Switzerland*
[3] *Swiss Nanoscience Institute, Klingelbergstrasse 82, 4056 Basel, Switzerland*
[4] *Department of Chemistry, Princeton University, Princeton, New Jersey 08544, USA*
[5] *Department of Physics, Northeastern University, Boston, Massachusetts 02115, USA*
[6] *Element Six, Harwell, OX11 0QR, United Kingdom*

(Dated: March 15, 2023)

Neutral silicon vacancy centers (SiV^0) in diamond are promising candidates for quantum applications; however, stabilizing SiV^0 requires high purity, boron doped diamond, which is not a readily available material. Here, we demonstrate an alternative approach via chemical control of the diamond surface. We use low-damage chemical processing and annealing in a hydrogen environment to realize reversible and highly stable charge state tuning in undoped diamond. The resulting SiV^0 centers display optically detected magnetic resonance and bulk-like optical properties. Controlling the charge state tuning via surface termination offers a route for scalable technologies based on SiV^0 centers, as well as charge state engineering of other defects.

Color centers in diamond are promising platforms for quantum information processing and quantum sensing. As atom-like systems, they can exhibit favorable properties such as long spin coherence times and narrow optical transitions [1–3]. Aside from their spin and orbital degrees of freedom, these color centers can often exhibit multiple stable charge states. The charge degree of freedom can be used as a powerful resource in spin-to-charge conversion and photoelectric detection [4, 5]. However, uncontrolled charge state conversion, especially near diamond surfaces, can also hinder applications and reduce the fidelity of quantum state manipulation [6]. It is therefore of great importance to gain understanding of the mechanisms for charge state conversion and develop methods to stabilize the desired charge state.

Recently, silicon vacancy (SiV) centers in diamond have emerged as a leading platform for quantum applications [7, 8]. SiV centers are known to exhibit two optically active charge states: negative (SiV^-) and neutral (SiV^0). As inversion-symmetric defects, both SiV^- and SiV^0 centers possess narrow, stable optical transitions [9, 10]. At liquid helium temperatures, SiV^- centers exhibit rapid spin decoherence [11, 12], while SiV^0 centers show long spin coherence times, making SiV^0 a more competitive platform [10, 13]. However, the fabrication of substrates with high conversion efficiency to SiV^0 is challenging. The neutral charge state is not stable in typical high-purity diamonds and requires pinning the Fermi level close to the valence band maximum (VBM) [14] while maintaining a high purity environment. Scalable fabrication of such substrates remains an outstanding challenge, and high conversion yield of SiV^0 has been restricted to a limited number of high purity, boron doped diamonds [10].

As an alternative approach to bulk doping, surface transfer doping in semiconductors like diamond [15] and silicon [16] enables tuning of the near-surface Fermi level, which strongly affects the properties of shallow color centers. For diamond, the electronic properties of its surface are known to depend strongly on the surface termination. Specifically, hydrogen-terminated (H-terminated) diamond exhibits a negative electron affinity, pulling the VBM above acceptor levels for surface adsorbates, which leads to a charge transfer process that in turn gives rise to Fermi level pinning near the VBM and band bending [17–19]. This surface transfer doping can be used to modulate the charge state of near-surface diamond defects. For example, the negative charge state of nitrogen vacancy (NV) centers was shown to be quenched under H-terminated surfaces [20], and active tuning of the NV charge state was demonstrated under H-terminated surfaces with electrolytic and in-plane gate electrodes [21–23]. Most prior demonstrations use plasma-based processes to prepare H-terminated surfaces, which can lead to degraded surface properties [24–26] and hydrogen decoration of shallow centers [27].

In this work, we demonstrate a new approach to stabilizing the neutral charge state of near-surface SiV centers in diamond by surface transfer doping. We develop a gentle, non-destructive, and robust approach of modifying the surface termination and realize reversible tuning of the charge state of SiV centers under different surface terminations. We show that the neutral charge state can be generated efficiently under H-termination while the negative charge state is more favorable under oxygen termination (O-termination). We observe bulk-like optical properties and optically detected magnetic resonance (ODMR) of SiV^0 centers under H-terminated surfaces,

paving the way for scalable fabrication of SiV^0 containing substrates in undoped diamond.

A high purity diamond grown by plasma chemical vapor deposition (Element Six "electronic grade") was used in the experiments. The diamond was polished into a 50 μm membrane and implanted with ^{28}Si at 25 keV with total fluence of 3×10^{11} cm^{-2}. The average depth of implanted Si is estimated to be 20 nm using stopping range in matter (SRIM) calculations (Fig. S1(a) [28]). The SiV centers were activated using high-temperature vacuum annealing [30]. We then fabricated parabolic reflectors (PR) with diameters of approximately 300 nm on the diamond membrane to enhance the collection efficiency [31]. The O-terminated surface was prepared with a refluxing mixture of concentrated perchloric, nitric, and sulfuric acids (tri-acid cleaning). The H-terminated surface was prepared by annealing the sample in either pure hydrogen at 750°C for 6 hours or in forming gas (5% H_2 in Ar) at 800°C for 72 hours [34, 35]. Measurements shown in the main text are based on samples prepared with the latter method. The SiV^0 measurements were conducted in a near-infrared confocal microscope at cryogenic temperatures. The SiV^- measurements were conducted in a visible wavelength confocal microscope at room temperature in ambient conditions. Optical emission was detected with either a spectrometer (Princeton Instruments Acton SP-2300i with Pixis 100 CCD and 300 grooves/mm grating) or a superconducting nanowire detector (Quantum Opus, optimized for 950 - 1100 nm). For more details of the experiments and sample preparation, see supplemental materials [28].

The dominant charge state of SiV centers is determined by the relative position between the Fermi level and SiV charge transition levels (Fig. 1(a)). The charge transition levels for SiV centers were calculated to be 0.25 eV above the VBM for $SiV^{+/0}$ and 1.43 eV above the VBM for $SiV^{0/-}$ [14, 36]. For an O-terminated surface, its positive electron affinity suppresses charge transfer to surface adsorbates [32, 37]. The Fermi level near the surface is dominated by nitrogen donors in the bulk (concentration below 5 ppb) that pin the Fermi level to 1.7 eV below the conduction band minimum (CBM) [38], and the negative charge state will be thermodynamically favored. Prior work on stabilizing the neutral charge state relies on boron doping [10], which pins the Fermi level at 0.37 eV above the VBM [39], in between $SiV^{0/-}$ and $SiV^{+/0}$. An alternative approach is to use high purity, undoped diamond with an H-terminated surface. For an H-terminated surface, charge transfer from the valence band to surface adsorbates leads to the accumulation of a two dimensional hole gas at the diamond surface, which pins the Fermi level to the VBM and results in upward band bending, pulling the $SiV^{0/-}$ charge transition point above the Fermi level [17–19]. With 5 ppb nitrogen as the dominant donor, the length scale of the band bending can extend beyond 50 nm [20].

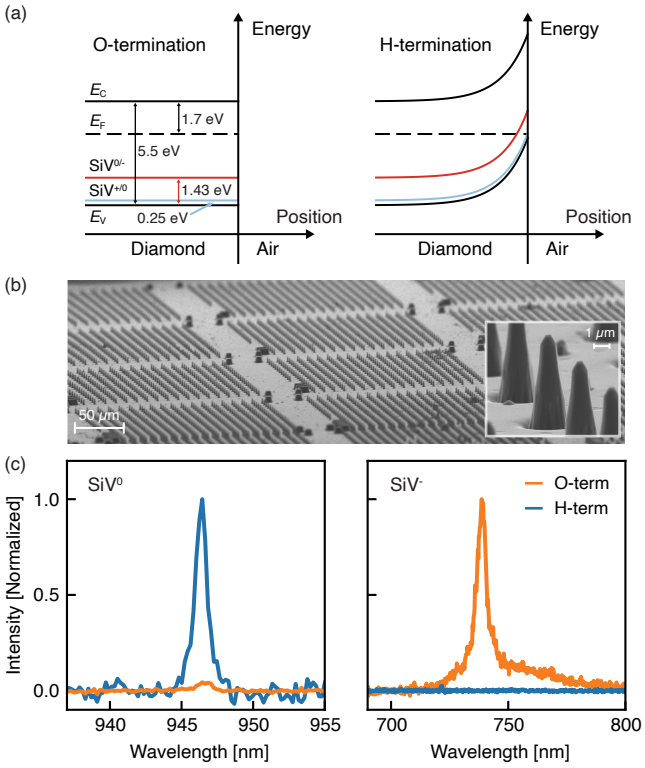

FIG. 1. **Charge state tuning of SiV centers via surface termination.** (a) Energy band diagram of diamond under different surface terminations. Under O-termination, the Fermi level is dominated by the nitrogen donors (with ionization energy of 1.7 eV) in the bulk. Under H-termination, upwards band bending occurs and the Fermi level near the diamond surface is pinned to the valence band maximum (E_V). E_C and E_F represent the positions of the conduction band minimum and Fermi level of diamond. The $SiV^{+/0}$ charge transition level (E_V + 0.25 eV) is shown as the blue curve, and the $SiV^{0/-}$ charge transition level (E_V + 1.43 eV) is shown as the red curve. (b) Scanning electron microscope (SEM) image of the PRs hosting the SiV centers (80° tilt). Inset: high resolution SEM of PRs. (c) Characteristic emission spectrum of SiV centers in a representative PR under different terminations. SiV^0 spectra were taken using 10 mW 857 nm excitation at 70 K. SiV^- spectra were taken with 0.1 mW 561 nm excitation at room temperature.

We study the charge state behavior of SiV centers in a membrane sample with a two dimensional array of PRs (Fig. 1(b)). Focusing on the photoluminescence spectrum of SiV centers in a particular PR, we observe that the emission spectrum changes drastically upon changing the chemical termination of the surface (Fig. 1(c)). Compared to the O-terminated surface, after H-termination we observe that the SiV^0 emission increases while the SiV^- emission decreases below background levels. We also observe formation of SiV^0 and quenching of SiV^- in unetched regions of the membrane under H-termination (Fig. S7 [28]). Our results are consistent with prior

work on H-terminated nanodiamonds where significant decrease in total SiV^- fluorescence is observed after H-termination via hydrogen plasma [40]. However, observing quenching of SiV^- alone is insufficient to prove the formation of SiV^0 because the window of stability for the neutral charge state is narrow [14], and the plasma treatment can lead to passivation of SiV centers [27], as well as surface degradation [24–26]. The observed emission intensity of SiV^0 formed under H-termination in the unetched region is within a factor of four of the emission intensity of SiV^0 prepared in a boron doped diamond with the same implantation dose, indicating that surface control is comparably effective to bulk doping (Fig. S8(a) [28]).

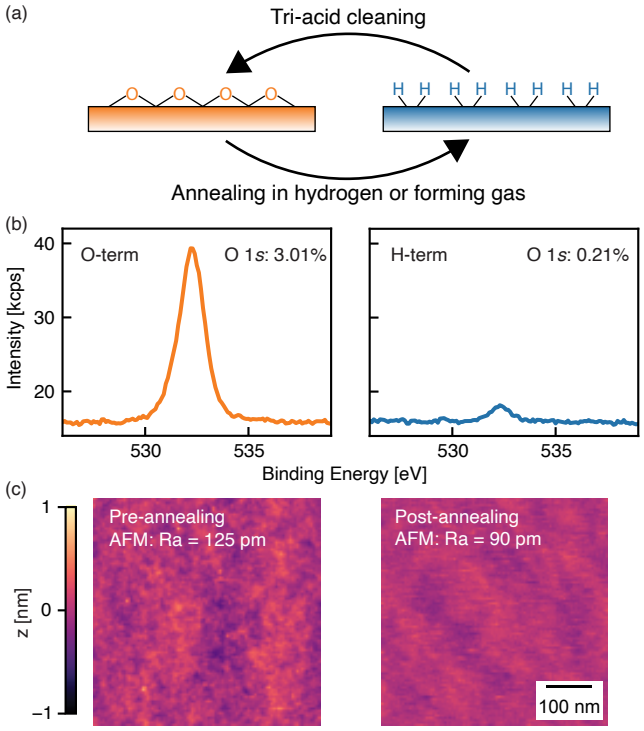

FIG. 2. **Characterization of the surface termination process.** (a) Schematic illustration of the surface termination process. The O-terminated surface is prepared using tri-acid cleaning. The H-terminated surface is prepared by annealing the sample in forming gas at 800°C for 72 hours or in hydrogen at 750°C for 6 hours. (b) XPS of the oxygen 1*s* peak in a test sample after the different processes. Hydrogen cannot be detected using XPS. Therefore, the absence of the oxygen 1*s* peak and any peaks other than the carbon 1*s* peak indicates the presence of H-termination. We measure XPS of the sample immediately after the processes to minimize contribution from contamination on the surface. (c) AFM scans of the surface of a test diamond before and after the annealing. The AFM scans were filtered to remove instrumental noise (Fig. S3 [28]). The surface morphology is unaffected by the annealing process.

In order to preserve the properties of near-surface color centers, it is important to use a gentle surface termination procedure that avoids subsurface damage and surface roughening. To prepare an H-terminated surface, we first ensure that the diamond surface is contamination free by tri-acid cleaning, and then we anneal the sample either in hydrogen or in forming gas (Fig. 2(a)). To remove the H-termination and reset the surface to O-termination, we perform tri-acid cleaning again. X-ray photoelectron spectroscopy (XPS) shows that the oxygen 1*s* peak intensity decreases after hydrogen termination (Fig. 2(b)). From the inelastic mean free path of photoelectrons and the X-ray energy (1487 eV), we estimate the contribution of the signal from a monolayer of atoms on diamond surface to be 7.6% [32, 41]. Based on the oxygen 1*s* signal intensity observed in XPS, we conclude that the surface has ∼40% of a monolayer of oxygen after tri-acid cleaning while the oxygen coverage is less than ∼3% of a monolayer after hydrogen termination. The sub-monolayer coverage of oxygen after tri-acid cleaning is consistent with previous observations [32]. This surface termination procedure is reversible and shows consistent results over many rounds of tri-acid cleaning and hydrogen termination (Fig. S2 [28]). Atomic force microscopy (AFM) scans before and after forming gas annealing reveal that the surface remains smooth (Fig. 2(c)), making the process compatible with shallow color center applications. This is in stark contrast to the commonly used hydrogen plasma treatment where significant surface roughening, subsurface damage, or hydrogen atom diffusion may occur during the plasma treatment [24–27].

We quantify the effect of surface termination on SiV centers by measuring spectral statistics across a large number of PRs. Histograms of the SiV^0 and SiV^- emission intensities are dramatically different under the two different surface terminations (Fig. 3(a)). Specifically, we observe that SiV^0 center emission is suppressed under O-termination while SiV^- center emission is suppressed under H-termination. We iteratively prepare the surface with O-termination and H-termination and observe reversible tuning between SiV^- and SiV^0. We observe that both the occurrence (Fig. 3(b)) and intensity (Fig. 3(c)) toggle reversibly for SiV^- and SiV^0 centers. This is in contrast to plasma-based processes, where diffusion of atomic hydrogen can lead to irreversible depletion of NV centers [27]. In addition, we probe the stability of the surface against cleaning in piranha solution (a 1:2 mixture of hydrogen peroxide in concentrated sulfuric acid) and long-term air exposure. The spectral statistics of SiV centers are unchanged upon piranha cleaning (Fig. S10 [28]). In fact, we note that initial observation of SiV^0 was under a surface prepared by annealing in hydrogen followed by more than 1.5 years of air exposure (Fig. S4 [28]). The stability of the charge state distribution against piranha cleaning and air exposure demonstrates the exceptional robustness of this approach.

Finally, we demonstrate that SiV^0 centers prepared

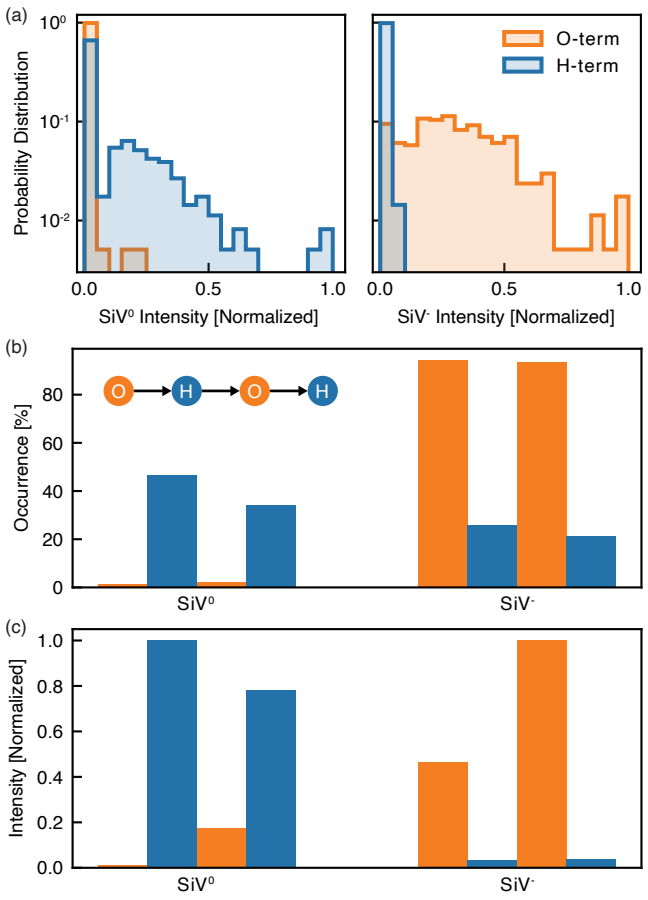

FIG. 3. **Statistics of SiV emission under different surface terminations.** (a) Left: SiV^0 emission intensity distribution under H- and O-termination measured at 10 K with 11 mW 857 nm excitation. Right: SiV^- emission intensity distribution under H- and O-termination measured in air with 0.1 mW 561 nm excitation. The intensities are extracted from Lorentzian fits of zero-phonon line intensities. Intensity for PRs without observable SiV emission is set to zero. (b) Occurrence (ratio of the number of PRs with SiV emission above the background to total number of PRs) of SiV^0 and SiV^- centers under different surface terminations. Orange denotes O-termination while blue denotes H-termination. Inset: the order of surface termination under study. (c) Average intensity of SiV^0 and SiV^- centers under different surface termination. SiV^0 emission is suppressed under O-termination while SiV^- emission is suppressed under H-termination. The PRs where no emission was identified are excluded from the analysis. SiV^- centers were measured using 1.88 mW 561 nm excitation for the first O-terminated surface while the power was kept at 0.1 mW for the rest of the measurements. The intensities are scaled by power.

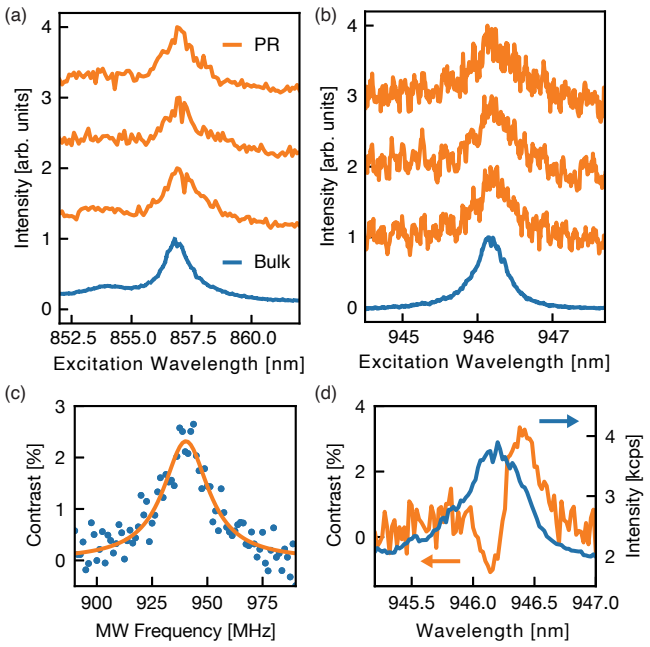

FIG. 4. **PLE and ODMR of SiV^0 under H-termination.** (a) PLE of the bound exciton transition on SiV^0 in three H-terminated PRs (orange) and a bulk-doped sample (blue). The excitation power is ∼10 mW. (b) PLE of the zero-phonon line transition of SiV^0 in three H-terminated PRs (orange) and a bulk-doped sample (blue). The PLE curves are background subtracted. The excitation power is ∼0.3 mW. The curves in (a) and (b) are offset from each other for clarity. (c) Continuous-wave ODMR of SiV^0 centers in a PR measured by exciting at 946.45 nm at 10 K. The orange curve shows a Lorentzian fit to the data. (d) Wavelength dependence of ODMR contrast (orange curve). Blue curve shows the PLE spectrum for comparison. ODMR was measured after H-termination and three piranha cleaning steps with the excitation power set to ∼25 μW.

under an H-terminated surface show similar properties to samples where SiV^0 centers are formed by bulk silicon doping during growth [10, 13]. We investigate the optical transitions of SiV^0 hosted in PRs prepared under an H-terminated surface using photoluminescence excitation (PLE) spectroscopy. First, we scan a narrow linewidth laser across one of the bound exciton transitions of SiV^0 [13] while monitoring the emission into the zero-phonon line (ZPL) at 946 nm. A resonance around 857 nm is observed, consistent with the spectrum from a bulk doped sample, as shown in Fig. 4(a). Then, we probe the ZPL transition by scanning a narrow linewidth laser across the SiV^0 ZPL while emission is measured at wavelengths longer than 960 nm. We observe a resonance at 946.2 nm, consistent with bulk PLE measurements (Fig. 4(b)).

We also observe ODMR in SiV^0 centers prepared under an H-terminated surface via excitation of the ZPL transition at 946.45 nm. As the microwave (MW) frequency is swept across the zero-field splitting of SiV^0, we observe a resonance peak at 940 MHz (Fig. 4(c)). The linewidth of ODMR at low powers (Fig. S12 and Fig. S13 [28]) is broader than previous observation [13], which is most likely related to the high density of SiV^0 in the current sample. In addition, we observe that the ODMR contrast

at the ZPL is strongly wavelength dependent (Fig. 4(d)), likely arising from fine structure in the ZPL that has been previously reported using optical spin polarization measurements [10, 42]. Even though individual transitions are not resolvable in PLE, they are spectrally separated enough to allow spin-dependent fluorescence. In our experiment, the narrowband laser can selectively excite one of the transitions, which produces strong spin polarization via either optical pumping from the finite cyclicity of the transitions or spin-dependent inter-system crossing. Therefore, by studying the ODMR contrast in a varying magnetic field, better understanding of SiV^0 excited state may be obtained. ODMR in SiV^0 centers via the ZPL transition, consistently observed across different samples (Fig. S14 [28]), is complementary to the recently demonstrated ODMR via the bound exciton transitions [13]. We note that in this sample the observed ODMR frequency of 940 MHz is slightly lower than the previously reported zero-field splitting [43], and the ODMR frequency shifts with higher optical excitation power and MW power (Fig. S12 and Fig. S13 [28]). The origin of the shift is currently under investigation, but we note that the sign of the shift is inconsistent with heating from the microwaves or laser [43].

In conclusion, we have demonstrated that chemical control of the diamond surface can be used to tune the charge state of SiV centers to stabilize the neutral charge state in undoped diamond. The gentle surface termination procedure we developed here allows for non-destructive, reversible and long-lived control of the diamond surface. Near-surface SiV^0 centers prepared using our approach preserve bulk-like optical properties and allow for optically detected magnetic resonance.

Our approach provides an alternative route to controlling color centers in diamond without careful control over the doping or defect states in the bulk. This approach is compatible with the fabrication of quantum photonics devices in diamond, where chemical processing and annealing procedures can be deployed after the fabrication of devices. In addition, the present work focuses on static stabilization of a particular charge state. Utilizing the surface termination to control the charge state may also be compatible with dynamic electric field tuning of the Fermi level, as has been demonstrated for NV centers with electrolytic and in-plane gate electrodes [21–23]. Such an approach could be widely applicable to other color centers in diamond. For example, Fermi level tuning via surface chemical control could help stabilize and identify other neutral group IV vacancy centers, or access additional charge states of SiV (SiV^+ and SiV^{2-}), whose spectroscopic signatures have been elusive [44, 45], possibly due to challenges in Fermi level engineering. Another avenue of exploration is to control the charge transfer process by using explicit electron acceptor materials on H-terminated diamond, for example molecular species (NO_2, C_{60} and O_3 [15, 46, 47]) or solid encapsulation materials such as transition metal oxides [48]. More broadly, surface transfer doping is applicable to other semiconductor materials such as silicon, gallium nitride and zinc oxide [16, 49]. Therefore, near-surface emitters in these materials may potentially also be tuned by similar surface control methods.

We gratefully acknowledge Z. Yuan for use of the visible wavelength confocal microscope and S. Mukherjee for help with surface characterization. Spectroscopy of SiV was supported by National Science Foundation through the Princeton Center for Complex Materials, a Materials Research Science and Engineering Center (Grant No. DMR-1420541) and the Air Force Office of Scientific Research under Grant No. FA9550-17-0158. Surface processing to control the charge state was supported by the U.S. Department of Energy, Office of Science, National Quantum Information Science Research Centers, Co-design Center for Quantum Advantage (C2QA) under contract number DE-SC0012704, the Swiss Nanoscience Institute and the quantERA grant SensExtreme. L.V.H.R. acknowledges support from the Department of Defense through the National Defense Science and Engineering Graduate Fellowship Program.

* npdeleon@princeton.edu

[1] W. B. Gao, A. Imamoglu, H. Bernien, and R. Hanson, Coherent manipulation, measurement and entanglement of individual solid-state spins using optical fields, Nature Photonics **9**, 363 (2015).

[2] D. D. Awschalom, R. Hanson, J. Wrachtrup, and B. B. Zhou, Quantum technologies with optically interfaced solid-state spins, Nature Photonics **12**, 516 (2018).

[3] M. Atatüre, D. Englund, N. Vamivakas, S.-Y. Lee, and J. Wrachtrup, Material platforms for spin-based photonic quantum technologies, Nature Reviews Materials **3**, 38 (2018).

[4] B. J. Shields, Q. P. Unterreithmeier, N. P. de Leon, H. Park, and M. D. Lukin, Efficient readout of a single spin state in diamond via spin-to-charge conversion, Phys. Rev. Lett. **114**, 136402 (2015).

[5] E. Bourgeois, A. Jarmola, P. Siyushev, M. Gulka, J. Hruby, F. Jelezko, D. Budker, and M. Nesladek, Photoelectric detection of electron spin resonance of nitrogen-vacancy centres in diamond, Nature Communications **6**, 8577 (2015).

[6] Z. Yuan, M. Fitzpatrick, L. V. H. Rodgers, S. Sangtawesin, S. Srinivasan, and N. P. de Leon, Charge state dynamics and optically detected electron spin resonance contrast of shallow nitrogen-vacancy centers in diamond, Phys. Rev. Research **2**, 033263 (2020).

[7] C. T. Nguyen, D. D. Sukachev, M. K. Bhaskar, B. Machielse, D. S. Levonian, E. N. Knall, P. Stroganov, R. Riedinger, H. Park, M. Lončar, and M. D. Lukin, Quantum network nodes based on diamond qubits with an efficient nanophotonic interface, Phys. Rev. Lett. **123**, 183602 (2019).

[8] M. K. Bhaskar, R. Riedinger, B. Machielse, D. S. Levonian, C. T. Nguyen, E. N. Knall, H. Park, D. Englund, M. Lončar, D. D. Sukachev, and M. D. Lukin, Experimental demonstration of memory-enhanced quantum communication, Nature **580**, 60 (2020).

[9] L. J. Rogers, K. D. Jahnke, T. Teraji, L. Marseglia, C. Müller, B. Naydenov, H. Schauffert, C. Kranz, J. Isoya, L. P. McGuinness, and F. Jelezko, Multiple intrinsically identical single-photon emitters in the solid state, Nature Communications **5**, 4739 (2014).

[10] B. C. Rose, D. Huang, Z.-H. Zhang, P. Stevenson, A. M. Tyryshkin, S. Sangtawesin, S. Srinivasan, L. Loudin, M. L. Markham, A. M. Edmonds, D. J. Twitchen, S. A. Lyon, and N. P. de Leon, Observation of an environmentally insensitive solid-state spin defect in diamond, Science **361**, 60 (2018).

[11] K. D. Jahnke, A. Sipahigil, J. M. Binder, M. W. Doherty, M. Metsch, L. J. Rogers, N. B. Manson, M. D. Lukin, and F. Jelezko, Electron–phonon processes of the silicon-vacancy centre in diamond, New Journal of Physics **17**, 043011 (2015).

[12] D. D. Sukachev, A. Sipahigil, C. T. Nguyen, M. K. Bhaskar, R. E. Evans, F. Jelezko, and M. D. Lukin, Silicon-vacancy spin qubit in diamond: A quantum memory exceeding 10 ms with single-shot state readout, Phys. Rev. Lett. **119**, 223602 (2017).

[13] Z.-H. Zhang, P. Stevenson, G. Thiering, B. C. Rose, D. Huang, A. M. Edmonds, M. L. Markham, S. A. Lyon, A. Gali, and N. P. de Leon, Optically detected magnetic resonance in neutral silicon vacancy centers in diamond via bound exciton states, Phys. Rev. Lett. **125**, 237402 (2020).

[14] A. Gali and J. R. Maze, Ab initio study of the split silicon-vacancy defect in diamond: Electronic structure and related properties, Phys. Rev. B **88**, 235205 (2013).

[15] P. Strobel, M. Riedel, J. Ristein, and L. Ley, Surface transfer doping of diamond, Nature **430**, 439 (2004).

[16] K. J. Rietwyk, Y. Smets, M. Bashouti, S. H. Christiansen, A. Schenk, A. Tadich, M. T. Edmonds, J. Ristein, L. Ley, and C. I. Pakes, Charge transfer doping of silicon, Phys. Rev. Lett. **112**, 155502 (2014).

[17] M. I. Landstrass and K. V. Ravi, Resistivity of chemical vapor deposited diamond films, Applied Physics Letters **55**, 975 (1989).

[18] F. Maier, M. Riedel, B. Mantel, J. Ristein, and L. Ley, Origin of surface conductivity in diamond, Physical Review Letters **85**, 3472 (2000).

[19] J. A. Garrido, S. Nowy, A. Härtl, and M. Stutzmann, The diamond/aqueous electrolyte interface: an impedance investigation, Langmuir **24**, 3897 (2008).

[20] M. V. Hauf, B. Grotz, B. Naydenov, M. Dankerl, S. Pezzagna, J. Meijer, F. Jelezko, J. Wrachtrup, M. Stutzmann, F. Reinhard, and J. A. Garrido, Chemical control of the charge state of nitrogen-vacancy centers in diamond, Phys. Rev. B **83**, 081304(R) (2011).

[21] B. Grotz, M. V. Hauf, M. Dankerl, B. Naydenov, S. Pezzagna, J. Meijer, F. Jelezko, J. Wrachtrup, M. Stutzmann, F. Reinhard, and J. A. Garrido, Charge state manipulation of qubits in diamond, Nature Communications **3**, 729 (2012).

[22] S. Karaveli, O. Gaathon, A. Wolcott, R. Sakakibara, O. A. Shemesh, D. S. Peterka, E. S. Boyden, J. S. Owen, R. Yuste, and D. Englund, Modulation of nitrogen vacancy charge state and fluorescence in nanodiamonds using electrochemical potential, Proceedings of the National Academy of Sciences **113**, 3938 (2016).

[23] M. V. Hauf, P. Simon, N. Aslam, M. Pfender, P. Neumann, S. Pezzagna, J. Meijer, J. Wrachtrup, M. Stutzmann, F. Reinhard, and J. A. Garrido, Addressing Single Nitrogen-Vacancy Centers in Diamond with Transparent in-Plane Gate Structures, Nano Letters **14**, 2359 (2014).

[24] B. Koslowski, S. Strobel, M. J. Wenig, and P. Ziemann, Roughness transitions of diamond(100) induced by hydrogen-plasma treatment, Applied Physics A: Materials Science and Processing **66**, 1159 (1998).

[25] A. Gaisinskaya, R. Edrei, A. Hoffman, and Y. Feldheim, Morphological evolution of polished single crystal (100) diamond surface exposed to microwave hydrogen plasma, Diamond and Related Materials **18**, 1466 (2009).

[26] K. G. Crawford, A. Tallaire, X. Li, D. A. Macdonald, D. Qi, and D. A. Moran, The role of hydrogen plasma power on surface roughness and carrier transport in transfer-doped H-diamond, Diamond and Related Materials **84**, 48 (2018).

[27] A. Stacey, T. J. Karle, L. P. McGuinness, B. C. Gibson, K. Ganesan, S. TomljenovicHanic, A. D. Greentree, A. Hoffman, R. G. Beausoleil, and S. Prawer, Depletion of nitrogenvacancy color centers in diamond via hydrogen passivation, Applied Physics Letters **100**, 071902 (2012).

[28] See Supplemental Material at [url] for experimental methods, additional characterization data and discussions, which includes Refs. [29–33].

[29] Y. Chu, N. de Leon, B. Shields, B. Hausmann, R. Evans, E. Togan, M. J. Burek, M. Markham, A. Stacey, A. Zibrov, A. Yacoby, D. Twitchen, M. Loncar, H. Park, P. Maletinsky, and M. Lukin, Coherent Optical Transitions in Implanted Nitrogen Vacancy Centers, Nano Letters **14**, 1982 (2014).

[30] R. E. Evans, A. Sipahigil, D. D. Sukachev, A. S. Zibrov, and M. D. Lukin, Narrow-linewidth homogeneous optical emitters in diamond nanostructures via silicon ion implantation, Phys. Rev. Applied **5**, 044010 (2016).

[31] N. Hedrich, D. Rohner, M. Batzer, P. Maletinsky, and B. J. Shields, Parabolic diamond scanning probes for single-spin magnetic field imaging, Phys. Rev. Applied **14**, 064007 (2020).

[32] S. Sangtawesin, B. L. Dwyer, S. Srinivasan, J. J. Allred, L. V. H. Rodgers, K. De Greve, A. Stacey, N. Dontschuk, K. M. O'Donnell, D. Hu, D. A. Evans, C. Jaye, D. A. Fischer, M. L. Markham, D. J. Twitchen, H. Park, M. D. Lukin, and N. P. de Leon, Origins of diamond surface noise probed by correlating single-spin measurements with surface spectroscopy, Phys. Rev. X **9**, 031052 (2019).

[33] U. F. S. D'Haenens-Johansson, A. M. Edmonds, B. L. Green, M. E. Newton, G. Davies, P. M. Martineau, R. U. A. Khan, and D. J. Twitchen, Optical properties of the neutral silicon split-vacancy center in diamond, Phys. Rev. B **84**, 245208 (2011).

[34] F. Fizzotti, A. Lo Giudice, C. Manfredotti, C. Manfredotti, M. Castellino, and E. Vittone, Diamond surface conductivity after exposure to molecular hydrogen, Diam. Relat. Mater. **16**, 836 (2007).

[35] V. Seshan, D. Ullien, A. Castellanos-Gomez, S. Sachdeva, D. H. Murthy, T. J. Savenije, H. A. Ahmad, T. S. Nunney, S. D. Janssens, K. Haenen, M. Nesládek, H. S. Van Der Zant, E. J. Sudhölter, and L. C. De Smet, Hydrogen termination of CVD diamond films by high-temperature annealing at atmospheric pressure, J. Chem. Phys. **138**,

10.1063/1.4810866 (2013).
[36] G. Thiering and A. Gali, Ab Initio Magneto-Optical Spectrum of Group-IV Vacancy Color Centers in Diamond, Phys. Rev. X **8**, 021063 (2018).
[37] F. Maier, J. Ristein, and L. Ley, Electron affinity of plasma-hydrogenated and chemically oxidized diamond (100) surfaces, Phys. Rev. B **64**, 165411 (2001).
[38] R. G. Farrer, On the substitutional nitrogen donor in diamond, Solid State Communications **7**, 685 (1969).
[39] R. M. Chrenko, Boron, the dominant acceptor in semiconducting diamond, Physical Review B **7**, 4560 (1973).
[40] L. J. Rogers, O. Wang, Y. Liu, L. Antoniuk, C. Osterkamp, V. A. Davydov, V. N. Agafonov, A. B. Filipovski, F. Jelezko, and A. Kubanek, Single Si-V^- centers in low-strain nanodiamonds with bulklike spectral properties and nanomanipulation capabilities, Phys. Rev. Applied **11**, 024073 (2019).
[41] H. Shinotsuka, S. Tanuma, C. J. Powell, and D. R. Penn, Calculations of electron inelastic mean free paths. X. Data for 41 elemental solids over the 50 eV to 200 keV range with the relativistic full Penn algorithm, Surface and Interface Analysis **47**, 871 (2015).
[42] B. L. Green, S. Mottishaw, B. G. Breeze, A. M. Edmonds, U. F. S. D'Haenens-Johansson, M. W. Doherty, S. D. Williams, D. J. Twitchen, and M. E. Newton, Neutral silicon-vacancy center in diamond: Spin polarization and lifetimes, Phys. Rev. Lett. **119**, 096402 (2017).
[43] A. M. Edmonds, M. E. Newton, P. M. Martineau, D. J. Twitchen, and S. D. Williams, Electron paramagnetic resonance studies of silicon-related defects in diamond, Phys. Rev. B **77**, 245205 (2008).
[44] V. S. Krivobok, E. A. Ekimov, S. G. Lyapin, S. N. Nikolaev, Y. A. Skakov, A. A. Razgulov, and M. V. Kondrin, Observation of a 1.979-eV spectral line of a germanium-related color center in microdiamonds and nanodiamonds, Physical Review B **101**, 144103 (2020).
[45] T. Lühmann, J. Küpper, S. Dietel, R. Staacke, J. Meijer, and S. Pezzagna, Charge-State Tuning of Single SnV Centers in Diamond, ACS Photonics **7**, 3376 (2020).
[46] H. Sato and M. Kasu, Maximum hole concentration for Hydrogen-terminated diamond surfaces with various surface orientations obtained by exposure to highly concentrated NO2, Diamond and Related Materials **31**, 47 (2013).
[47] M. Kubovic and M. Kasu, Enhancement and stabilization of hole concentration of hydrogen-terminated diamond surface using ozone adsorbates, Japanese Journal of Applied Physics **49**, 110208 (2010).
[48] S. A. O. Russell, L. Cao, D. Qi, A. Tallaire, K. G. Crawford, A. T. S. Wee, and D. A. J. Moran, Surface transfer doping of diamond by MoO3: A combined spectroscopic and Hall measurement study, Applied Physics Letters **103**, 202112 (2013).
[49] V. Chakrapani, C. Pendyala, K. Kash, A. B. Anderson, M. K. Sunkara, and J. C. Angus, Electrochemical Pinning of the Fermi Level: Mediation of Photoluminescence from Gallium Nitride and Zinc Oxide, J. Am. Chem. Soc. **130**, 12944 (2008).